J. Org. Chem. **2001,** *66,* 2005−2010

Theoretical Study of Nucleophilic Substitution at Two-Coordinate Sulfur

Steven M. Bachrach*,[†] and BettyCep D. Gailbreath[‡]

Department of Chemistry, Trinity University, 715 Stadium Drive, San Antonio, Texas 78212, and
Department of Chemistry, Northern Illinois University, DeKalb, Illinois 60115

sbachrach@trinity.edu

Received October 10, 2000

A series of nucleophilic substitution reactions involving simple species (chloride, phosphide, methoxide, hydroxide, and amide) as nucleophile and leaving group in methylsulfenyl derivatives were examined at B3LYP/aug-cc-pVDZ. The reactions involving hydroxide and amide correspond to deprotonation and not substitution. The substitution reactions follow an addition−elimination pathway, possessing a triple-well potential energy surface. The intermediate along this pathway is of trigonal bipyramid geometry with the nucleophile and leaving group occupying apical positions.

Nucleophilic substitution reactions play a central role in both synthetic chemistry and in the development of mechanistic paradigms.[1] While most attention has centered on substitution at carbon, there is growing interest for substitution at heteroatoms.

Experimental studies of nucleophilic substitution at dicoordinate sulfur reveal a mechanistic dependence on the nucleophile and the leaving group. Ciuffarin's group has examined nucleophilic substitution of sulfenyl halides and thiocyanates with amines and alcohols.[2−4] The relative reaction rates, they argued, are best understood via an addition−elimination mechanism. They proposed an intermediate where the nucleophile and leaving group occupy the apical positions of a trigonal bipyramid centered on sulfur. Kice and co-workers have examined nucleophilic substitution at sulfenyl, sulfinyl, and sulfonyl centers.[5−8] Generally, they too conclude that substitution at the sulfenyl center proceeds with the formation of an intermediate. However, thiolate and cyanide attack of the sulfenyl center of phenyl benzenethiosulfonate shows evidence of an S_N2 mechanism. Extensive examination of the disulfide−thiolate interchange supports an S_N2 mechanism, based on β_{nuc} values from a Bronsted plot and kinetic and thermodynamic data.[9−15]

Bachrach and Mulhearn recently examined the gas-phase thiolate−disulfide exchange[16] and the reaction of thiolate with trisulfides[17] using ab initio methods. At the HF level, these reactions appear to follow an S_N2 pathway: a single transition state is found connecting an entrance and exit ion−dipole complex. However, when a correlated wave function is used (MP2, MP4, or CCSD(T)), the shape of the potential energy surface (PES) radically alters. Instead of the classic gas-phase double-well potential of an S_N2 reaction, a triple-well potential is found. The thiolate nucleophile and either di- or trisulfide first combine without a barrier to form an ion dipole complex. Next, the nucleophile attacks the sulfur through an asymmetric TS to form a stable intermediate whose structure is very similar to the HF TS. In transiting the exit channel, the leaving group departs through a TS leading to another ion−dipole complex.

We recently described the reaction of chloride ion with SCl_2 via high-level theoretical methods and gas-phase experiments.[18] The potential energy surface for this reaction has no transition states; rather, the two reagents fall into a single-well conforming to SCl_3^-.

In this paper, we report density functional calculations examining the reaction of nucleophilic substitution of methylsulfenyl derivatives using simple nucleophiles and leaving groups. As long as the nucleophile is not too strong a base (where deprotonation is the only reaction observed), the nucleophilic substitution proceeds along an addition−elimination pathway.

Computational Methods

The reactions examined here are listed in Scheme 1. The first five reactions are identity reactions, while the last two involve cases where the incoming nucleophile differs from the leaving group.

[†] Trinity University.

[‡] Northern Illinois University.

(1) Lowry, T. H.; Richardson, K. S. *Mechanism and Theory in Organic Chemistry,* 3rd ed.; Harper and Row: New York, 1987.

(2) Ciuffarin, E.; Guaraldi, G. *J. Org. Chem.* **1970**, *35*, 2006−2010.

(3) Ciuffarin, E.; Griselli, F. *J. Am. Chem. Soc.* **1970**, *92*, 6015−6019.

(4) Senatore, L.; Ciuffarin, E.; Sagramora, L. *J. Chem. Soc. B* **1971**, 2191−2193.

(5) Kice, J. L.; Large, G. B. *J. Am. Chem. Soc.* **1968**, *90*, 4069−4076.

(6) Kice, J. L.; Rogers, T. E.; Warheit, A. C. *J. Am. Chem. Soc.* **1974**, *96*, 8020−8026.

(7) Kice, J. I.; Rogers, T. E. *J. Org. Chem.* **1976**, *41*, 225−227.

(8) Kice, J. I.; Liu, C.-C. *J. Org. Chem.* **1979**, *44*, 1918−1923.

(9) Whitesides, G. M.; Lilburn, J. E.; Szajewski, R. P. *J. Org. Chem.* **1977**, *42*, 332.

(10) Wilson, J. M.; Bayer, R. J.; Hupe, D. J. *J. Am. Chem. Soc.* **1977**, *99*, 7922−7926.

(11) Freter, R.; Pohl, E. R.; Hupe, D. J. *J. Org. Chem.* **1979**, *44*, 1771−1774.

(12) Szajewski, R. P.; Whitesides, G. M. *J. Am. Chem. Soc.* **1980**, *102*, 2011.

(13) Whitesides, G. M.; Houk, J.; Patterson, M. A. K. *J. Org. Chem.* **1983**, *48*, 112−115.

(14) Hupe, D. J.; Pohl, E. R. *Isr. J. Chem.* **1985**, *26*, 395−399.

(15) Singh, R.; Whitesides, G. M. *J. Am. Chem. Soc.* **1990**, *112*, 1190−1197.

(16) Bachrach, S. M.; Mulhearn, D. C. *J. Phys. Chem.* **1996**, *100*, 3535−3540.

(17) Mulhearn, D. C.; Bachrach, S. M. *J. Am. Chem. Soc.* **1997**, *118*, 99415-9421.

(18) Gailbreath, B. D.; Pommerening, C. A.; Bachrach, S. M.; Sunderlin, L. S. *J. Phys. Chem. A* **2000**, *104*, 2958−2961.

10.1021/jo001463q CCC: $20.00

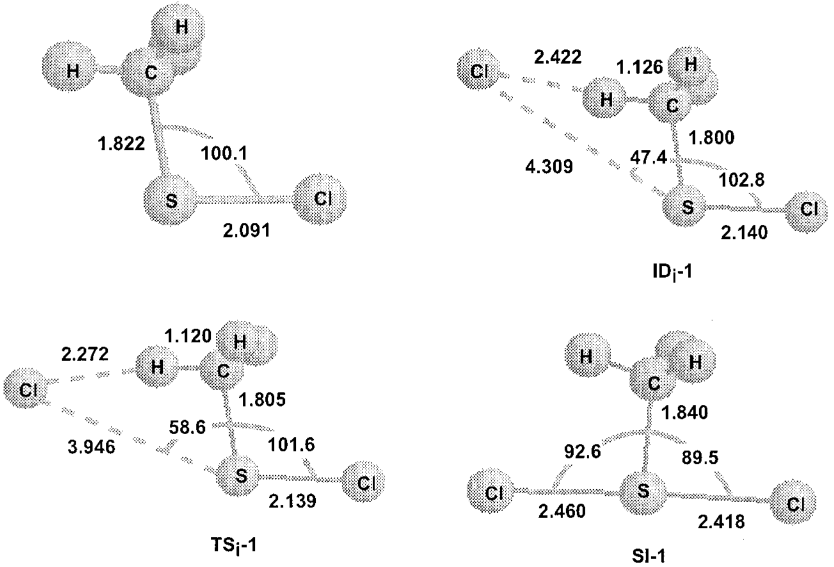

Figure 1. Geometries of critical points along reaction 1. All distances are in Å, and all angles are in deg.

Scheme 1

$Cl^- + MeS\text{-}Cl \rightarrow Cl\text{-}SMe + Cl^-$	Reaction 1
$PH_2^- + MeS\text{-}PH_2 \rightarrow PH_2\text{-}SMe + PH_2^-$	Reaction 2
$MeO^- + MeS\text{-}OMe \rightarrow MeO\text{-}SMe + MeO^-$	Reaction 3
$MeO^- + i\text{PrS-OMe} \rightarrow \text{MeO-S-}i\text{Pr} + MeO^-$	Reaction 3’
$HO^- + MeS\text{-}OH \rightarrow HO\text{-}SMe + HO^-$	Reaction 4
$NH_2^- + MeS\text{-}NH_2 \rightarrow NH_2\text{-}SMe + NH_2^-$	Reaction 5
$Cl^- + MeS\text{-}OMe \rightarrow Cl\text{-}SMe + MeO^-$	Reaction 6
$Cl^- + MeS\text{-}OH \rightarrow Cl\text{-}SMe + HO^-$	Reaction 7

All structures of reactants, transition states, intermediates, and products for reactions 1−7 were completely optimized at B3LYP/aug-cc-pVDZ[19−22] using GAUSSIAN-98.[23] Since the topology of the potential energy surface is dependent on the computational level,[16] the choice of method is critical. Extensive comparison of the potential energy surface for simple thiolate-disulfide reactions ($HS^- + HSSH$, $HS^- + CH_3SSH$, $CH_3S^- + HSSCH_3$) show a triple-well potential for all three reactions at MP2, MP4, CCSD(T), B3LYP, BPW91, and MPW1PW91 using a variety of different basis sets that all include at least one set of polarization functions and one set of diffuse functions.[16,24] Therefore, since the DFT methods are computationally advantageous and provide reliable results in an analogous reaction, we choose to utilize it in this study.

The nature of all structures was confirmed using analytical frequencies; all ground states had only real frequencies and all transition states had one and only one imaginary frequency. Zero-point energies were scaled by 0.980.[25] Gibbs free energies are calculated at STP. For all the reactions examined, the only significant difference between the relative electronic and free energies is the stabilization of the reactants relative to the other critical points by about 6 kcal mol^{-1}, attributable to the bimolecular character of the reactants and the unimolecular character of the other points. We will primarily discuss the electronic energies.

Results

Reaction 1. The potential energy surface for reaction 1 (and also reactions 2 and 3′) is demarked by five critical points, corresponding to an incoming ion−dipole complex (**ID$_i$-1**), an incoming transition state (**TS$_i$-1**), a stable intermediate (**SI-1**), an outgoing transition state (**TS$_o$-1**), and last an outgoing ion−dipole complex (**ID$_o$-1**). Due to the symmetry of the reaction, the incoming and outgoing TSs and IDs are identical.

The optimized structures of these compounds are drawn in Figure 1. In forming the ion−dipole complex **ID$_i$-1**, the incoming chloride ion interacts with a hydrogen atom of the methyl group. The chloride is 2.422 Å from the hydrogen and 4.309 Å from the sulfur atom. The reaction progresses by having the chloride swing down toward the sulfur, forming **TS$_i$-1**; the S−Cl distance decreases to 3.946 Å and the Cl−S−C angle widens from 47.4° to 58.6°, yet a Cl−H interaction remains. Continuing on, the chloride moves toward sulfur and away from the methyl hydrogen, reaching the stable intermediate **SI-1**. This intermediate possesses two long S−Cl distances (2.460 Å to the incoming Cl and 2.418 Å to the leaving Cl) and the Cl−S−Cl angle is nearly linear (177.9°). There is, in fact, one more transition structure on the surface. Note that the S−Cl distances are not identical in **SI-1** and that one of the methyl hydrogens is nearly coplanar with the entering chlorine, sulfur and carbon. A transition state of Cs symmetry connects the entrance and exit stable intermediate. It lies only 0.03 kcal mol^{-1} above **SI-1** and actually is 0.03 kcal mol^{-1}

---

[19] Becke, A. D. *J. Chem. Phys.* **1993**, *98*, 5648−5650.

[20] Lee, C.; Yang, W.; Parr, R. G. *Phys. Rev. B* **1988**, *37*, 785−789.

[21] Dunning, T. H. J. *J. Chem. Phys.* **1989**, *90*, 1007−1023.

[22] Woon, D.; Dunning, T. H. J. *J. Chem. Phys.* **1993**, *98*, 1358−1371.

[23] Frisch, M. J.; Trucks, G. W.; Schlegel, H. B.; Scuseria, G. E.; Robb, M. A.; Cheeseman, J. R.; Zakrzewski, V. G.; Montgomery, J. A. J.; Stratmann, R. E.; Burant, J. C.; Dapprich, S.; Millam, J. M.; Daniels, A. D.; Kudin, K. N.; Strain, M. C.; Farkas, O.; Tomasi, J.; Barone, V.; Cossi, M.; Cammi, R.; Mennucci, B.; Pomelli, C.; Adamo, C.; Clifford, S.; Ochterski, J.; Petersson, G. A.; Ayala, P. Y.; Cui, Q.; Morokuma, K.; Malick, D. K.; Rabuck, A. D.; Raghavachari, K.; Foresman, J. B.; Cioslowski, J.; Ortiz, J. V.; Baboul, A. G.; Stefanov, B. B.; Liu, G.; Liashenko, A.; Piskorz, P.; Komaromi, I.; Gomperts, R.; Martin, R. L.; Fox, D. J.; Keith, T.; Al-Laham, M. A.; Peng, C. Y.; Nanayakkara, A.; Gonzalez, C.; Challacombe, M.; Gill, P. M. W.; Johnson, B.; Chen, W.; Wong, M. W.; Andres, J. L.; Gonzalez, C.; Head-Gordon, M.; Replogle, E. S.; Pople, J. A. *GAUSSIAN-98*; rev. A.7; Gaussian, Inc.: Pittsburgh, PA, 1998.

[24] Bachrach, S. M.; Dao, T.; Mynar, J. Manuscript in preparation.

[25] Wong, M. H. *Chem. Phys. Lett.* **1996**, *256*, 391−399.

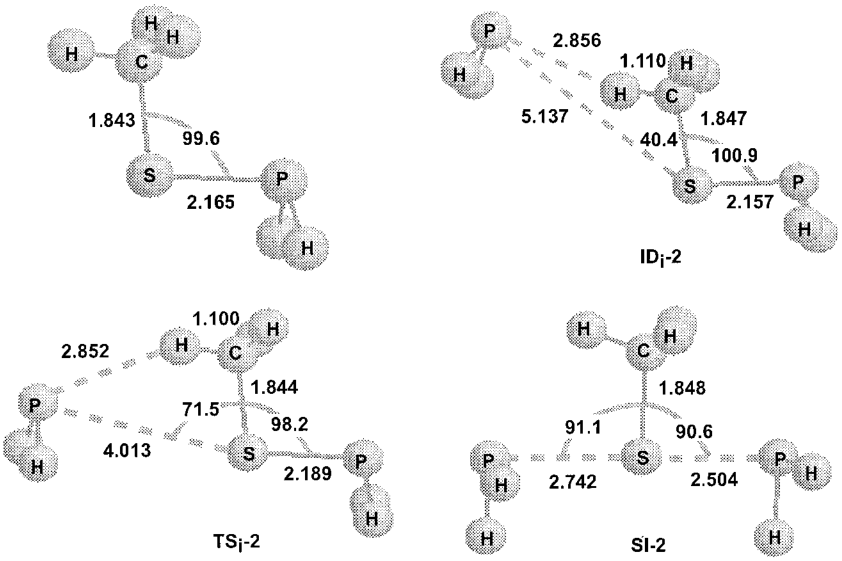

Figure 2. Geometries of critical points along reaction 2. All distances are in Å, and all angles are in deg.

Table 1. Relative Energies[a] and Gibbs Free Energies[b] (kcal mol^{-1}) for Reactions 1, 2, 3′, 6, and 7

rxn	reactants	ID_i	TS_i	INT	TS_o	ID_o	products
1	0.0	−13.33	−13.16	−21.77	−13.16	−13.33	0.0
	0.0	*−7.47*	*−6.22*	*−15.12*	*−6.22*	*−7.47*	*0.0*
2	0.0	−6.04	−5.02	−5.88	−5.02	−6.04	0.0
	0.0	*0.32*	*2.98*	*1.54*	*2.98*	*0.32*	*0.0*
3′	0.0	−16.83	−14.80	−24.96	−14.80	−16.83	0.0
	0.0	*−7.44*	*−6.20*	*−15.78*	*−6.20*	*−7.44*	*0.0*
6	0.0	−8.90	−8.00	−8.51			+41.61
	0.0	*−3.28*	*−1.02*	*−2.32*			*+38.72*
7	0.0	−9.07	−8.20	−8.67			+47.78
	0.0	*−3.40*	*−1.28*	*−2.43*			*+46.34*

[a] Evaluated at B3LYP/aug-cc-pVDZ + ZPE scaled by 0.980. [b] Relative free energies evaluated at 1 atm and 298.15 K, listed in italics.

Table 2. Experimental[26] Gas-Phase Deprotonation Energies (DPE, kcal mol^{-1})

compd	DPE	compd	DPE
NH_3	399.6	PH_3	369.0
H_2O	390.8	HCl	333.4
CH_3OH	379.2	CH_3SCH_3	390.2

more stable than the intermediate when ZPE is included. Since the surface is so flat in this regime, we will consider the stable intermediate here (and for all reactions) as just the single structure and neglect the TS connecting the two intermediates.

The relative energies of the critical points along reaction 1 are listed in Table 1. The ion−dipole complex lies 13.33 kcal mol^{-1} below reactants. The barrier for reaction is only 0.17 kcal mol^{-1}, with the intermediate lying 21.77 kcal mol^{-1} below reactants or 8.44 kcal mol^{-1} below **ID$_i$-1**. The very small barrier coupled with the very low energy of the intermediate inspired our search for a stable hypercoordinate sulfur species, which we found in SCl_3^-.[18] The same trend is observed using the Gibbs free energies, except that the reactants are stabilized by about 6 kcal mol^{-1} relative to the other critical points.

Reaction 2. Figure 2 displays the structures of the critical points on the PES of reaction 2. Their relative energies are listed in Table 2. PH_2- and CH_3PH_2 combine without a barrier to form **ID$_i$-2**, with a release of 6.04 kcal mol^{-1}. The distance between the two fragments is quite large—the P−H interaction distance is 2.856 Å and the P−S distance is extremely long, 5.137 Å. The transition state **TS$_i$-2** is reached when the PH_2 moiety swings down toward sulfur (with little change of the P−H distance), reaching a P−S distance of 4.013 Å. The P−S−P angle is 169.7°. The barrier height is 0.98 kcal mol^{-1}. The intermediate **SI-2** is characterized by long S−P distances (2.742 and 2.504 Å) and a near-linear P−S−P angle. The intermediate lies 5.88 kcal mol^{-1} below reactants, but 0.16 kcal mol^{-1} above **ID$_i$-2**. Relative differences in free energy of the critical points parallel the electronic energies, however all the critical point are higher than reactants.

Reaction 3. Reaction 3 is the identity reaction of methoxide with CH_3S-OCH_3. We were unable to locate a transition state that corresponded to nucleophilic substitution. Rather, the only TS located was for deprotonation, i.e., $CH_3O^- + CH_3S-OCH_3 \rightarrow CH_3OH + {}^-CH_2SOCH_3$. Alkyl substitution of the methyl group may reduce its acidity. We next examined the reaction of methoxide with $CH_3CH_2S-OCH_3$ but again could only locate a transition state for deprotonation. However, we could locate the appropriate substitution TS for the reaction of methoxide with $(CH_3)_2CHS-OCH_3$, reaction 3′.

The geometries of the critical points for reaction 3′ are drawn in Figure 3, and their relative energies are listed in Table 1. The ion−dipole complex **ID$_i$-3′** is considerably more stable than reactants (16.83 kcal mol^{-1} below reactants), resulting from a hydrogen bond between the methoxy oxygen and the methinyl hydrogen. **TS$_i$-3′** is 2.03 kcal mol^{-1} above **ID$_i$-3′**, with a slightly longer O−H hydrogen bond and much shorter O−S interaction (3.256 Å in **TS$_i$-3′** vs 3.724 Å in **ID$_i$-3′**). The intermediate is 10.16 kcal mol^{-1} below the TS, over 8 kcal mol^{-1} more stable than **ID$_i$-3′**. The two S−O distances are very similar, differing by only 0.014 Å, and the O−S−O angle is 174.5°.

Reactions 4 and 5. Reactions 4 and 5 involve attack with nucleophiles that are also relatively strong bases. Given the difficulties described for locating the proper TS with methoxide as a nucleophile, we anticipated further difficulties with these reactions. Numerous attempts at locating **ID$_i$-4** and **ID$_i$-5** resulted in structures

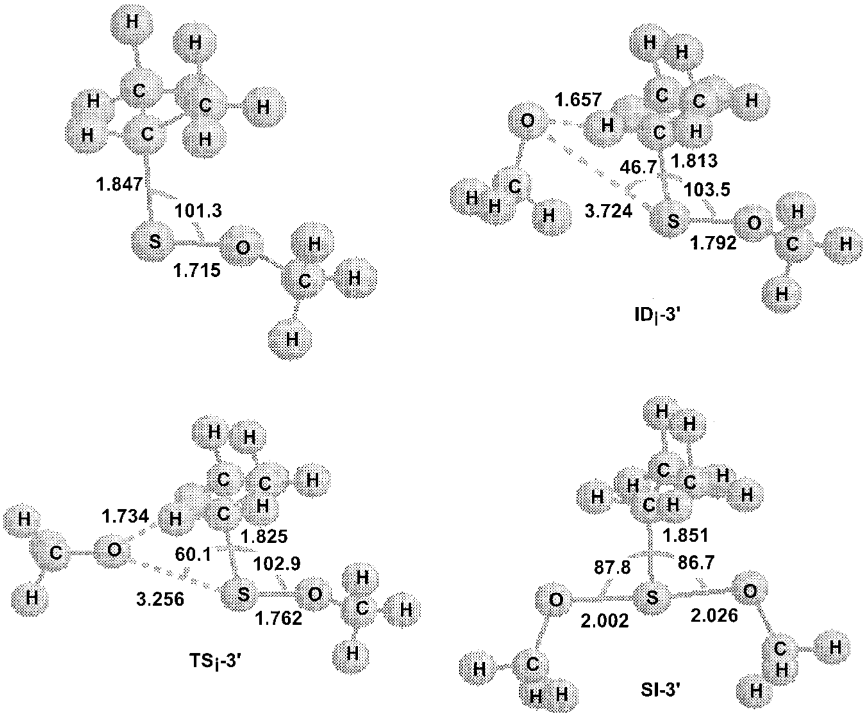

Figure 3. Geometries of critical points along reaction 3′. All distances are in Å, and all angles are in deg.

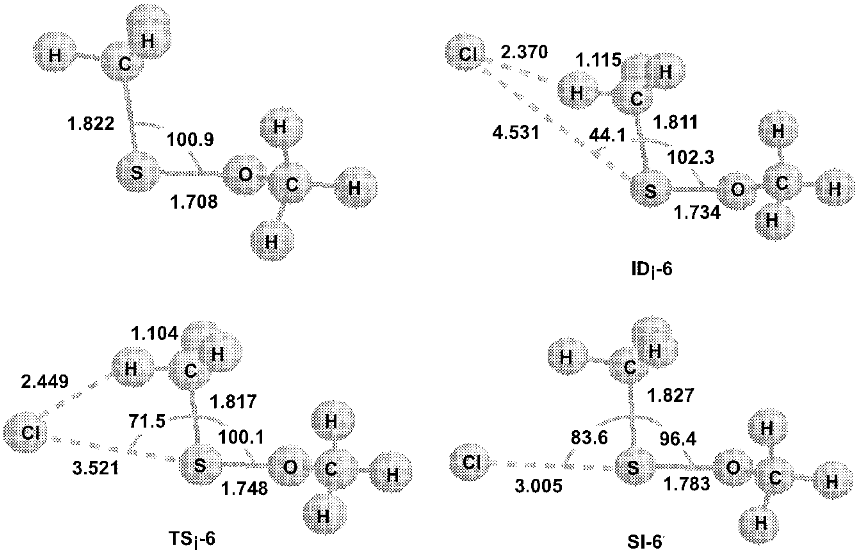

Figure 4. Geometries of critical points along reaction 6. All distances are in Å, and all angles are in deg.

where a hydrogen transferred from the methyl group to the base. The only TSs located corresponded to proton transfer. Since hydroxide is a weaker base than amide, we opted to do further exploration of a possible substitution pathway for Reaction 4. Attempts were made to locate ion dipole complexes and transition states for reactions of hydroxide with CH_3CH_2SOH and $(CH_3)_2$-CHSOH. In both cases, the only TSs obtained were for proton transfer, removing the methylenyl or methinyl proton, respectively. Last, we examined the reaction with $(CH_3)_3CSOH$, assuming that the acidity would be sufficiently reduced here that a substitution pathway could be found. However, deprotonation off a methyl group was again found, presumably in this case leading toward an elimination product. No further analogues of Reactions 4 and 5 were investigated.

Reactions 6 and 7. Reactions 6 and 7 are nonidentity nucleophilic substitution reactions. Both involve chloride as the nucleophile, but differ in their leaving groups, methoxide in reaction 6 and hydroxide in reaction 7. Both are very endothermic; the reaction energy for reaction 6 is +41.61 kcal mol^{-1}, and as expected since hydroxide is a stronger base than methoxide, reaction 7 is 6.17 kcal mol^{-1} more endothermic.

Entrance ion−dipole complexes, transition states and intermediates for both reactions were located and are displayed in Figures 4 and 5. Reaction energetics are indicated in Table 1. Both reactions possess relatively flat PESs. The three critical points lie within 0.90 kcal mol^{-1} for reaction 6 and 0.87 kcal mol^{-1} for reaction 7.

Repeated attempts were made to locate exit ion−dipole complexes and transition states for both reactions. We

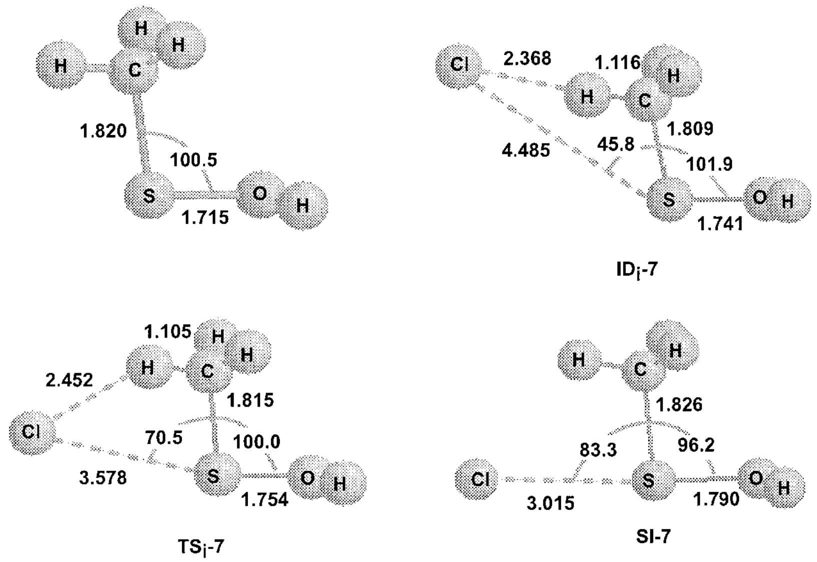

Figure 5. Geometries of critical points along reaction 7. All distances are in Å, and all angles are in deg.

were able to locate only proton-transfer pathways. Replacing the methyl group attached to sulfur with an ethyl or isopropyl group did not alter the surface and again only proton transfer was observed. Apparently, both methoxide and hydroxide are simply too strong bases to observe substitution chemistry in these systems. It is interesting to note that these substitution reactions are exceedingly endothermic (41.61 kcal mol^{-1} and 47.78 kcal mol^{-1} for reactions 6 and 7, respectively), which also contributes toward the difficulty in locating this pathway.

Discussion

A major complication met within this study was the propensity for deprotonation when the nucleophile instead acts as a base. The experimental gas-phase acidities[26] of the conjugate acids of the nucleophiles studied are listed in Table 2. Since the DPE of dimethyl sulfide is 390.2 kcal mol^{-1}, it is not surprising that both amide and hydroxide prefer to deprotonate rather than substitute. The other nucleophiles are sufficiently less acidic than methyl sulfide, and we can therefore obtain substitution pathways.

Reactions 1, 2, and 3′ all possess a triple-well potential energy surface, each with a single intermediate and an entrance and exit ion−dipole complex and TS. This surface is consistent with an addition−elimination pathway and distinctly incompatible with an S_N2 mechanism, which must not involve an intermediate. The same is also true for the first half of reactions 6 and 7. Here, the nucleophile (Cl^-) adds to sulfur through an asymmetric transition state forming an intermediate. The second half of the addition−elimination pathway (the elimination step) does not occur since the leaving groups, methoxide in reaction 6 and hydroxide in reaction 7, are very strong bases.

The structures of the intermediates share a major common feature. The angles formed by the nucleophile, sulfur, and leaving group are nearly linear: 177.9° in **SI-1**, 178.3° in **SI-2**, 174.5° in **SI-3′**, 179.5° in **SI-6**, and 178.9° in **SI-7**. This is consistent with Ciuffarin's trigonal bipyramid model,[2,3] having sulfur's two lone-pairs occupying equatorial positions. This structure is also consistent with an addition−elimination process.

Table 3. NPA[28] Charges[a] in the Intermediates

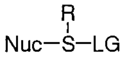

$$\mathrm{Nuc{-}\overset{R}{\overset{|}{S}}{-}LG}$$

compd	S	Nuc	LG	R
SI-1	0.182	−0.540	−0.570	−0.072
SI-2	−0.127	−0.479	−0.295	−0.100
SI-3′	0.379	−0.623	−0.626	−0.111
SI-6	0.450	−0.878	−0.472	−0.101
SI-7	0.419	−0.880	−0.441	−0.099

[a] These charges are the sum of the atomic charges for all atoms within the substituent group.

While the reactions are all consistent with the addition−elimination pathway, their PESs show differing well depths and barrier heights. Reactions 1 and 3′ are dominated by very stable intermediates. The transition states for these two reactions are early, as seen by the relatively small differences in the geometries of the ion−dipoles and transition states; mainly just a swing of the nucleophile down from the methyl group by about 15° converts the ID into the TS. This early TS is consistent with the Hammond Postulate.[27] The critical points for the other reactions are energetically very close, implying (by the Hammond Postulate) later TSs than in the previous two examples. These TSs are reached from the IDs by having the nucleophile swing away from the methyl group by about 30° along with a significant decrease in the sulfur-nucleophile distance.

The stability of the intermediate can be rationalized in terms of the degree of charge delocalization. Table 3 presents the NPA[28] charges on the groups present in the intermediates. The very stable intermediates (**SI-1** and **SI-3′**) are characterized by large negative charges on the nucleophile and leaving group. The charge is therefore extensively delocalized in these two intermediates, leading to their stability. The extreme case is our previous

---

(26) Linstrom, P. J.; Mallard, W. G. *NIST Chemistry Webbook*, 2000, URL: http://webbook.nist.gov/.

(27) Hammond, G. S. *J. Am. Chem. Soc.* **1955**, *77*, 334.

(28) Reed, A. E.; Weinstock, R. B.; Weinhold, F. *J. Chem. Phys.* **1985**, *83*, 735.

study of SCl_3^-, where the PES has no barriers or complexes; the global minimum is the analogous intermediate.[18]

While there is extensive charge-transfer evident in **SI-2** (0.52 e have moved off the incoming nucleophile), the net charge distribution is not as delocalized as in **SI-1** and **SI-3′**, as evidenced by the difference in charges on the nucleophile and leaving group. Even less charge transfer occurs in **SI-6** and **SI-7**. In these two cases, just over 0.1 e are moved off the incoming chloride ion and the resulting charge delocalization is small. Therefore, these intermediate do not possess the great stabilization found in **SI-1** nor **SI-3′**.

Last, the charge distributions shed some light on the β_{nuc} values obtained in a number of solution-phase studies.[9−11] Values of β_{nuc} range from −0.3 to −0.5 for the thiolate-disulfide exchange and have been interpreted as showing large negative charge on the nucleophile and leaving group. The NPA charges in the intermediates indicate large negative charges on the nucleophile and leaving group, consistent with the experimental results, without invoking an S_N2 mechanism.

Conclusion

For all five nucleophilic substitution reactions examined here (including the half-reaction of reactions 6 and 7), the mechanism is addition−elimination. The PES is characterized by its three wells, corresponding to entrance ion−dipole complex, intermediate, and exit ion−dipole complex. Even though the surface is somewhat flat for reactions 2, 6, and 7, there definitely is a transition state connecting the entrance ion−dipole with the intermediate, critical points that are incompatible with an S_N2 mechanism. The intermediate has the nucleophile and leaving group in the apical positions, as expected for a trigonal bipyramid structure. These results are in accord with our earlier examination of thiolate substitution of di- and trisulfides.[16,17] These theoretical studies also agree with previous experimental solution-phase studies[2−8] that suggest that nucleophilic substitution at dicoordinate sulfur proceeds via an addition−elimination mechanism.

Acknowledgment is made to the donors of the Petroleum Research Fund, administered by the American Chemical Society, and to the Robert A. Welch Foundation for partial support of this research. B.D.G. is grateful for financial support provided by the Northern Illinois University Graduate School through a Dissertation Completion Award.

JO001463Q